



# Effects of 3-methyladenine, an autophagy inhibitor, on the elevated blood pressure and arterial dysfunction of angiotensin II-induced hypertensive mice

Youngin Kwon, Chae Eun Haam, Seonhee Byeon, Soo-Kyoung Choi<sup>\*</sup>, Young-Ho Lee<sup>\*</sup>

Department of Physiology, College of Medicine, Brain Korea 21 PLUS Project for Medical Sciences, Yonsei University, 50 Yonsei-ro, Seodaemun-gu, Seoul 03722, the Republic of the Korea

## ARTICLE INFO

### Keywords:

Autophagy  
Mesenteric artery  
Angiotensin II  
Hypertension  
Endothelium-dependent relaxation  
Nitric Oxide

### Chemical compounds studied in this article:

3-methyladenine (PubChem CID: 135398661)  
angiotensin II (PubChem CID: 172198)  
N $\omega$ -nitro-L-arginine (PubChem CID: 4367)  
acetylcholine (PubChem CID: 6060)  
phenylephrine (PubChem CID: 5284443)  
U-46619 (PubChem CID: 5311493)  
indomethacin (PubChem CID: 3715)  
sodium nitroprusside (PubChem CID: 11953895)

## ABSTRACT

Autophagy is an intracellular degradation system that disassembles cytoplasmic components through autophagosomes fused with lysosomes. Recently, it has been reported that autophagy is associated with cardiovascular diseases, including pulmonary hypertension, atherosclerosis, and myocardial ischemia. However, the involvement of autophagy in hypertension is not well understood. In the present study, we hypothesized that excessive autophagy contributes to the dysfunction of mesenteric arteries in angiotensin II (Ang II)-induced hypertensive mice. Treatment of an autophagy inhibitor, 3-methyladenine (3-MA), reduced the elevated blood pressure and wall thickness, and improved endothelium-dependent relaxation in mesenteric arteries of Ang II-treated mice. The expression levels of autophagy markers, beclin1 and LC3 II, were significantly increased by Ang II infusion, which was reduced by treatment of 3-MA. Furthermore, treatment of 3-MA induced vasodilation in the mesenteric resistance arteries pre-contracted with U46619 or phenylephrine, which was dependent on endothelium. Interestingly, nitric oxide production and phosphorylated endothelial nitric oxide synthase (p-eNOS) at S1177 in the mesenteric arteries of Ang II-treated mice were increased by treatment with 3-MA. In HUVECs, p-eNOS was reduced by Ang II, which was increased by treatment of 3-MA. 3-MA had direct vasodilatory effect on the pre-contracted mesenteric arteries. In cultured vascular smooth muscle cells (VSMCs), Ang II induced increase in beclin1 and LC3 II and decrease in p62, which was reversed by treatment of 3-MA. These results suggest that autophagy inhibition exerts beneficial effects on the dysfunction of mesenteric arteries in hypertension.

## 1. Introduction

Hypertension is defined as a lasting increase in systolic blood pressure  $\geq 130$  mmHg or diastolic pressure  $\geq 80$  mmHg and one of the most important risk factors for stroke, heart failure, myocardial infarction, and chronic kidney disease [1]. There are various contributors to hypertension such as vascular hypertrophy, increased peripheral vascular resistance, and endothelial dysfunction [2]. Peripheral resistance is determined by several factors, including vascular reactivity which is controlled by endothelium-dependent relaxation [3]. The vascular endothelium plays an important role in the regulation of vascular tone by releasing vasodilatory substances such as nitric oxide (NO),

prostacyclin (prostaglandin I<sub>2</sub>, PGI<sub>2</sub>), endothelium derived hyperpolarizing factor (EDHF) and vasoconstrictor substances such as thromboxane (TXA<sub>2</sub>), and endothelin-1 (ET-1). Several studies have suggested that impaired endothelium-dependent vasodilation is associated with the pathogenesis of cardiovascular diseases including atherosclerosis, systemic and pulmonary hypertension [4].

Autophagy is an intracellular degradation system that involves the delivery of cytoplasmic constituents to the lysosome. It is essential for cell survival, differentiation, development, and homeostasis. In the process of autophagy, cells form double-membrane vesicles called autophagosomes that fuse with the lysosome to degrade the materials it contains [5]. Although many proteins and genes are involved in the

**Abbreviations:** Ang II, angiotensin II; RAS, renin-angiotensin system; Atg, autophagy-related; PI3K, class III phosphatidylinositol 3-kinase; VSMCs, vascular smooth muscle cells; HUVECs, Human umbilical vein endothelial cells; K-H, Krebs-Henseleit; L-NNA, N $\omega$ -nitro-L-arginine; AVOs, acidic vesicular organelles; W/O, wash out; W/L ratio, wall thickness/lumen diameter ratio; Veh, vehicle;  $\alpha$ -SMA,  $\alpha$ -smooth muscle actin; PE, phenylephrine; 3-MA, 3-methyladenine.

<sup>\*</sup> Corresponding authors.

E-mail addresses: [skchoi@yuhs.ac](mailto:skchoi@yuhs.ac) (S.-K. Choi), [yhlee@yuhs.ac](mailto:yhlee@yuhs.ac) (Y.-H. Lee).

<https://doi.org/10.1016/j.bioph.2022.113588>

Received 3 July 2022; Received in revised form 17 August 2022; Accepted 17 August 2022

Available online 19 August 2022

0753-3322/© 2022 The Authors. Published by Elsevier Masson SAS. This is an open access article under the CC BY-NC-ND license (<http://creativecommons.org/licenses/by-nc-nd/4.0/>).

autophagy process, in the present study, we discuss three substances that are important in autophagic flux: beclin1, microtubule-associated protein 1A/1B-light chain 3 (LC3), and ubiquitin-binding protein p62 (p62). Beclin1 is a core component of the class III phosphatidylinositol 3-kinase (PI3K) complex, which promotes phagophore nucleation. The class III PI3K complex produces phosphatidylinositol-3-phosphate on the phagophore membrane to recruit autophagy-related (Atg) proteins involved in autophagosome formation [6]. The ubiquitin-like LC3 is involved in the elongation of the phagophore. LC3 II is a membrane-bound form that is modified through the conjugation of phosphatidylethanolamine to the carboxyl glycine. LC3 II is integrated into the growing phagophore and remains an autophagosome membrane until autolysosomes [7]. The adapter molecule, p62/sequestosome 1, has a multi-domain that comprises a ubiquitin-binding domain and an LC3-interacting region. It binds with ubiquitinated cargoes and then delivers them to autophagosomes [8]. A group of PI3K inhibitors such as wortmannin, LY294002, and 3-methyladenine are well known as autophagy inhibitors based on their inhibitory effect on class III PI3K activity [9]. Among these autophagy inhibitors, 3-methyladenine has been widely used in animal studies and has shown significant effects on various animal models of diseases including cerebral infarction, stroke, lung injuries, and osteoarthritis [10–13].

It has been well known that excessive and uncontrolled autophagy may cause cell death and senescence by leading to the depletion of essential molecules and organelles [14]. Previous studies showed that impaired autophagy contributes to premature vascular aging in hypertension and atherosclerosis and pulmonary hypertension [15]. Moreover, in vivo and in vitro studies have shown that angiotensin II (Ang II) contributes toward inducing autophagy in cardiomyocytes, cardiac fibroblasts, podocytes, endothelial cells, and vascular smooth muscle cells [16–21] and administration of autophagy inhibitors or LC3 gene silencing reduces elevated arterial pressure in spontaneously hypertensive rats [22]. Although previous studies have suggested the association between autophagy and hypertension, the involvement of autophagy in vascular dysfunction related with hypertension has not been characterized.

In the present study, we hypothesized that excessive autophagy might be involved in the progression of Ang II-induced hypertension. Moreover, inhibition of autophagy may ameliorate vascular dysfunction in Ang II-induced hypertension. In order to study this, we used an autophagy inhibitor, 3-methyladenine, which is a well-known autophagy inhibitor that inhibits the formation of autophagosomes through the inhibitory effect of PI3K [23].

## 2. Materials and methods

### 2.1. Animals

All experiments were performed according to the Guide for the Care and Use of Laboratory Animals published by US National Institutes of Health (NIH publication no. 85-23, 2011) and were approved by the Ethics Committee and the Institutional Animal Care and Use Committee of Yonsei University, College of Medicine (Approval number: 2019-0308). Animals were housed in individually ventilated caging system cages and in controlled conditions with light-dark cycle of 12:12 h, 50 ± 10 % humidity, and 22 ± 2 °C. Animals had food pellets and water ad libitum.

### 2.2. Animal models and tissue preparation

Eight-week-old male C57BL/6 mice were anesthetized with oxygen and 1.5–2.5 % inhalational isoflurane throughout surgery. We used surgical scissors to create an approximately 1 cm incision in the mid-scapular region to implant an osmotic mini-pump (model 2004; Alzet, Cupertino, CA, USA). Mini-pumps were loaded with either Ang II (Merck, Burlington, MA, USA) dissolved in saline or saline (vehicle)

alone. Ang II was infused at 1000 ng/kg/min for 4 weeks and the treatment of 3-methyladenine was initiated when Ang II treatment was started. The mice were randomized into four groups: (i) vehicle-treated mice; (ii) vehicle-treated mice that received an autophagy inhibitor (3-methyladenine, 30 mg/kg/day by intraperitoneal injection); (iii) Ang II-treated mice; and (iv) Ang II-treated mice that received 3-methyladenine. Ten mice were used for each group. After 4 weeks of Ang II infusion, the mice were anesthetized through respiratory anesthesia using 1.5–2.5 % isoflurane, and then euthanized by cardiac excision. The arteries were immediately excised and placed in chilled Krebs-Henseleit (K-H) solution [composed of (in mol/L) NaCl, 119; KCl, 4.6; CaCl<sub>2</sub>, 2.5; MgSO<sub>4</sub>, 1.2; KH<sub>2</sub>PO<sub>4</sub>, 1.2; NaHCO<sub>3</sub>, 25; glucose, 11.1 (Sigma-Aldrich, St. Louis, MO, USA)]. The adipose tissues and connective tissues were removed under an optical microscope (model SZ-40, Olympus, Shinjuku, Tokyo, Japan). To study direct effect of 3-methyladenine on the pre-contracted arteries, 10-week old male C57BL/6 mice were used.

### 2.3. Blood pressure measurements

Systolic blood pressure was measured in 7- to 12-week-old mice using the tail-cuff method with a photoplethysmography blood pressure monitoring system (BP-2000, Visitech Systems, Apex, NC, USA) as previously described [24]. Before the implantation of a mini-pump, the mice were trained using the blood pressure monitoring device for 1 week. On each measurement day, 10 readings were obtained from each mouse.

### 2.4. Functional studies

The segment of the second branch mesenteric artery (130–200 µm in inner diameter) was cannulated on glass micropipettes in a Pressure Servo System PS/200 (Living Systems Instrumentation, Burlington, VT, USA). The heated K-H solution was superfused to the vessel chamber continuously to maintain a temperature of 37 °C. During the 30-min equilibration period, the pressure was maintained at 40 mmHg using pressure-servo control perfusion systems. The lumen diameter was measured using the Soft Edge Acquisition Subsystem (IonOptix, Milton, MA, USA). Isometric tension was recorded on the mesenteric arteries in a wire myograph (Danish Myo Technology, Aarhus, Denmark). The mesenteric arteries were set to a basal force of 2 mN. The data were recorded and analyzed using LabChart7 (ADInstruments, Dunedin, New Zealand). All mesenteric arteries were initially contracted with high K<sup>+</sup> solution (7 × 10<sup>-2</sup> mol/L KCl in K-H solution). To further contract the mesenteric arteries, we used phenylephrine (10<sup>-5</sup> mol/L; α1-adrenergic receptor agonist; Sigma-Aldrich), U46619 (10<sup>-7</sup> mol/L or 10<sup>-6</sup> mol/L; thromboxane A<sub>2</sub> receptor agonist; Cayman Chemicals, Ann Arbor, MI, USA), and high K<sup>+</sup> solution. 3-methyladenine was purchased from Sigma-Aldrich and Cayman Chemicals. The arteries were pre-contracted with phenylephrine and endothelium-dependent relaxation was measured in response to cumulative doses of acetylcholine (10<sup>-9</sup>–10<sup>-5</sup> mol/L, Sigma-Aldrich). The endothelium-denuded arteries were confirmed by the absence of response to acetylcholine. A nitric oxide donor, sodium nitroprusside dihydrate (SNP, Sigma-Aldrich) was used as a vasodilator.

### 2.5. Western blot analysis

Western blotting was performed in the aortas, mesenteric arteries, vascular smooth muscle cells (VSMCs), and human umbilical endothelial cells (HUVECs). All the samples were homogenized in ice-cold RIPA buffer (radioimmunoprecipitation assay buffer; Sigma-Aldrich) with complete protease and phosphatase inhibitor cocktail (Thermo Scientific, Waltham, MA, USA). After lysis, tissue debris was removed by centrifugation, and cleared protein lysates were used. The samples were loaded in 8–15 % SDS-PAGE gels. The separated proteins were transferred to nitrocellulose membranes. The membranes were incubated

with primary antibodies against the following antigens: Beclin1 (1:4000, #3738S, Cell Signaling, Boston, MA, USA), LC3 (1:4000, #4108S, Cell Signaling), p62 (1:4000, ab109012, Abcam, Cambridge, MA, USA), p-eNOS (S1177, 1:1000, MA5-14957, Invitrogen, Carlsbad, CA, USA), total eNOS (1:1000, PA1-037, Invitrogen), and  $\beta$ -actin (1:5000, ab3280, Abcam). HRP-conjugated anti-rabbit (31450, Merck) and anti-mouse (12349, Merck) secondary antibodies were used. To ensure equal loading control of eNOS, the membranes were stripped with reblot solution (Restore™ Western Blot Stripping Buffer, Thermo Scientific) and re-probed with total eNOS antibody after p-eNOS was measured.

## 2.6. Immunofluorescence staining

Beclin1 expression in the mesenteric arteries was measured by using immunofluorescence staining. The vessels were cleaned of fat and connective tissues and cut into 4–5 mm thick sections. The cleaned arteries were immediately embedded in OCT and frozen in liquid nitrogen. The frozen Section (5  $\mu$ m) were serially collected and blocked with PBS containing 3 % bovine serum albumin. After blocking, the arteries were incubated with beclin1 (1:100, ab62557, Abcam) and smooth muscle actin (1:100, ab7817, Abcam) for 1 h at room temperature. Streptavidin-conjugated Alexa Fluor 488 (1:100, A21202, Invitrogen) and Alexa Fluor 594 (1:100, A21207, Invitrogen) secondary antibodies were used for 1 h at room temperature in the dark. DAPI was used for nuclear staining (Vector Laboratories, Burlingame, CA, USA). Immunofluorescence images were obtained using a laser scanning confocal microscope (LSM700, Carl Zeiss, Oberkochen, Germany). Immunofluorescence intensity was quantified using Image J (National Institutes of Health, Bethesda, MD, USA).

## 2.7. Acridine orange staining

Acridine orange is a lysosomotropic dye used to stain acidic vesicular organelles [25]. The VSMCs were subcultured in 12 mm coverslips with poly L-lysine coating. After starvation for 24 h, VSMCs were incubated in a serum-free medium treated with Ang II or co-treated with Ang II and 3-methyladenine for 24 h, exposed to acridine orange (1  $\mu$ g/mL) for 15 min, and then washed with PBS. After fixation with 4 % paraformaldehyde, VSMCs were examined under a laser scanning confocal microscope (Carl Zeiss) with a 60 $\times$  water immersion objective. The excitation/emission wavelengths for green and red fluorescence were 488/518 nm and 555/573 nm, respectively.

## 2.8. RNA preparation and real-time PCR

Total RNA was isolated from the aortas using an RNA extraction kit (GeneAll Biotechnology Co. Ltd, Seoul, Korea). The isolated RNA (1  $\mu$ g) was used to synthesize complementary DNA (cDNA) using a cDNA synthesis kit (Takara Bio, Shiga, Japan). Final primer concentration was 0.4  $\mu$ M. Real-time PCR was performed with SYBR Green (Takara) using a Step-One Plus System (Applied Biosystems, Foster City, CA, USA) and run by triplicate in the same PCR plate. The following primers were used for the reaction: mouse p62 forward 5'-GTC AAG ATG GAG CCG GAG AA-3'; mouse p62 reverse 5'-CGG GTC GAG CGA GTC CTT-3'; mouse actin forward 5'-AAA TCG TGC GTG ACA TCA AAG A-3'; and mouse actin reverse 5'-GCC ATC TCC TGC TCG AAG TCT-3'. The reaction conditions were as follows: initial denaturation at 95 °C for 30 s, 40 amplification cycles at 95 °C for 5 s, and 60 °C for 30 s. The relative amount of p62 mRNA was calculated by using the  $2^{-\Delta\Delta CT}$  (CT, comparative threshold cycle) method.  $\Delta\Delta CT$  was calculated using the following formula:  $\Delta\Delta CT = (CT_{p62} - CT_{actin})_{Ang\ II} - (CT_{p62} - CT_{actin})_{vehicle}$ .

## 2.9. Determination of nitric oxide levels

Nitric oxide production in mesenteric arteries was measured as

previously described [26]. The mesenteric arteries were incubated in 4-amino-5-methylamino-2', 7'-difluorofluorescein diacetate (DAF-FM diacetate,  $5 \times 10^{-6}$  mol/L; Cayman Chemicals) and acetylcholine ( $10^{-6}$  mol/L; for 30 min at 37 °C in K-H solution). The arteries were washed with the K-H solution and images were acquired using an Olympus BX51 microscope (Olympus). The fluorescent images were analyzed using Image J software (National Institutes of Health).

## 2.10. Cell culture

Aortic VSMCs were obtained from 8-week-old male Sprague-Dawley rats. The rats were anesthetized by oxygen and 5 % inhalational isoflurane using isoflurane vaporizer (Vapor 19.3; Drager, Lubeck, Germany), and then euthanized by cardiac excision. The thoracic aorta was removed and placed in Dulbecco's modified Eagle medium (DMEM; Gibco, Life Technologies, Carlsbad, CA, USA). After removing the connective tissues, the aorta was transferred to an enzyme dissociation mixture containing DMEM with 1 mg/mL collagenase (Activity:  $\geq 125$  units/mg, Worthington, Lakewood, NJ, USA) and 0.5 mg/mL elastase (Activity:  $\geq 8$  units/mg, Worthington) with subsequent removal of adventitia. The suspension was centrifuged, and the pellet was resuspended in DMEM supplemented with 10 % FBS and 1 % penicillin/streptomycin solution. HUVECs were obtained from the American Type Culture Collection (ATCC, Rockville, MD, USA) and cultured in vascular cell basal medium (ATCC) supplemented with Endothelial Cell Growth Kit-BBE (ATCC). Cultured cells from passages 3–5 were used.

## 2.11. Statistical analysis

All in vitro, ex vivo, and in vivo experiments were performed in a blinded and randomized manner at least 5 independent experiments. All results were expressed as mean  $\pm$  SEM. Statistical analysis was performed using GraphPad Prism (Version 7, GraphPad software, La Jolla, CA, USA). Comparisons among groups were analyzed by two-way ANOVA with the Tukey's post hoc analysis; post hoc tests were run only when F achieved  $p < 0.05$ . The concentration-response curve was fitted to sigmoidal curve with a variable slope using four parameters logistic equation in GraphPad Prism.

## 3. Results

### 3.1. Effect of 3-methyladenine on blood pressure in Ang II-induced hypertensive mice

To investigate the involvement of autophagy in blood pressure regulation, we measured systolic blood pressure in Ang II-induced hypertensive mice using the tail-cuff method. The systolic blood pressure of Ang II-treated mice was significantly increased compared with that of vehicle-treated mice. Injection of an autophagy inhibitor, 3-methyladenine, significantly reduced the blood pressure of Ang II-treated mice (vehicle,  $114.8 \pm 0.8$  mmHg; vehicle + 3-methyladenine,  $107.5 \pm 5.0$  mmHg; Ang II,  $181.0 \pm 6.2$  mmHg; Ang II + 3-methyladenine,  $134.4 \pm 5.5$  mmHg; at the end of experiments, Fig. 1A). The dose of 3-methyladenine was determined with references to previous studies [27,28]. There were no differences in body weight among groups (vehicle,  $29.3 \pm 0.8$  g; vehicle + 3-methyladenine,  $27.6 \pm 0.8$  g; Ang II,  $27.0 \pm 0.6$  g; Ang II + 3-methyladenine,  $26.2 \pm 0.8$  g; at the end of experiments, Fig. 1B). We analyzed the structure of the mesenteric arteries by measuring the lumen diameter and wall thickness at resting pressure (40 mmHg) in K-H solution (active diameter). We found that wall thickness of mesenteric arteries was increased in the Ang II-treated mice compared to vehicle-treated mice. Treatment with 3-methyladenine decreased the wall/lumen ratio of the mesenteric arteries compared with Ang II-treated mouse mesenteric arteries (Fig. 1C–E).

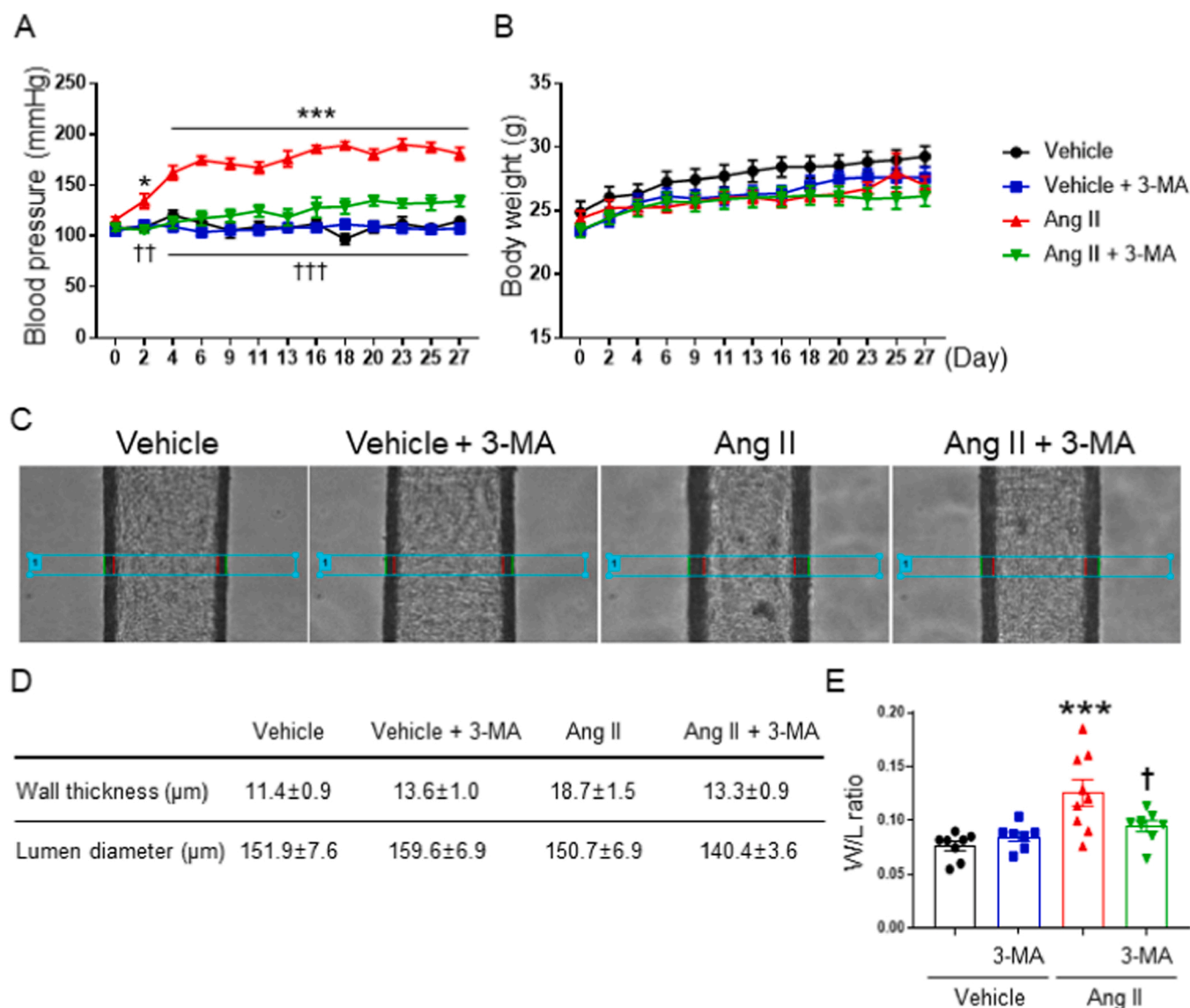


**Fig. 1.** Effects of an autophagy inhibitor, 3-methyladenine, on blood pressure, body weight, and wall thickness of mesenteric arteries. (A) Blood pressure and (B) body weight in vehicle- and Ang II-treated (with or without 3-methyladenine) mice.  $n = 8$  for Vehicle, Vehicle + 3-MA, and Ang II + 3-MA.  $n = 9$  for Ang II. (C) Representative images of the mesenteric arteries in resting state (40 mmHg). (D and E) Wall/lumen ratio was measured from 7 randomly selected mouse mesenteric arteries for each independent groups. Data are shown as means  $\pm$  SEM. The  $n$ -values mean number animals.  $*p < 0.05$ ,  $***p < 0.001$  for Vehicle vs. Ang II,  $\dagger p < 0.05$ ,  $\dagger\dagger p < 0.01$ , and  $\dagger\dagger\dagger p < 0.001$  for Ang II vs. Vehicle + Ang II. (3-MA: 3-methyladenine; W/L ratio: wall thickness/lumen diameter ratio).

### 3.2. Effects of 3-methyladenine on the expression levels of autophagic markers in the mesenteric arteries and aortas of Ang II-induced hypertensive mice

To explore whether autophagy level was changed in the vessels of Ang II-induced hypertension and treatment of 3-methyladenine affected autophagy level, we performed western blot analysis with the mesenteric arteries and aortas. We found that the expression levels of autophagy markers, beclin1, LC3 II, and p62, were increased in Ang II-treated mice, which was reduced by treatment of 3-methyladenine (Fig. 2A and B). To support the western blot analysis data, we performed immunofluorescence staining analysis for beclin1 in the mesenteric arteries. Consistent with the western blotting results, the immunostaining data indicated that the expression level of beclin1 was increased in the mesenteric arteries of Ang II-treated mice, which was reduced by treatment with 3-methyladenine (Fig. 2C).

It is known that p62 is usually reduced when autophagy is increased. However, we observed that p62 level was increased in the vessels of Ang

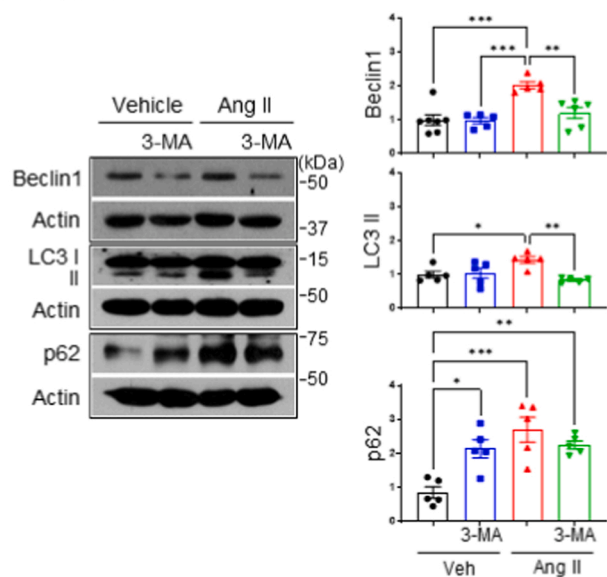
II-induced hypertensive mice. Thus, to clarify the increased expression of p62 in Ang II-treated mice, we examined the time-dependent effects of Ang II infusion on p62 levels. During the 1-week infusion, the level of p62 was decreased in the aortas. However, chronic infusion of Ang II increased p62 levels (Fig. 2D). To strengthen the western blot analysis data, we measured the mRNA levels of p62 in the aortas of Ang II-treated mice. The gene expression of p62 was upregulated in mice infused with Ang II for 4 weeks compared with vehicle-treated mice (Fig. 2E).

### 3.3. Effects of 3-methyladenine on endothelium-dependent relaxation in the mesenteric arteries of Ang II-induced hypertensive mice

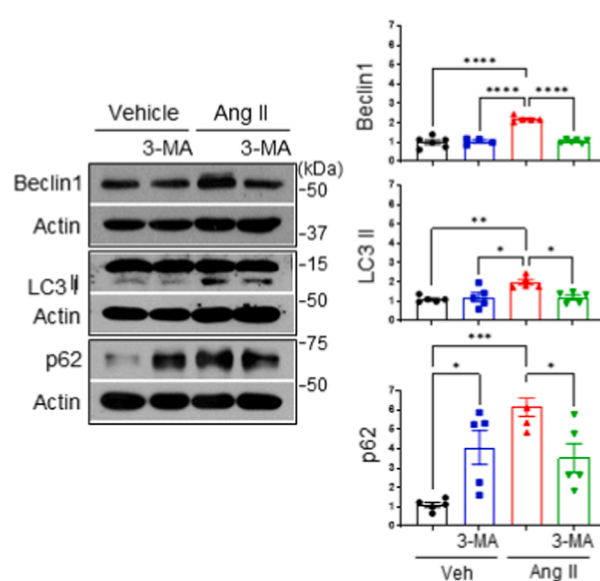
In order to find out which mechanism is involved in the effect of 3-methyladenine on the blood pressure reduction, we measured vascular reactivity in the mesenteric arteries of Ang II-infused and vehicle-treated mice. Endothelium-dependent relaxation was significantly reduced in Ang II-infused mice compared with vehicle-treated mice (Fig. 3A and C). The treatment of 3-methyladenine improved endothelium-



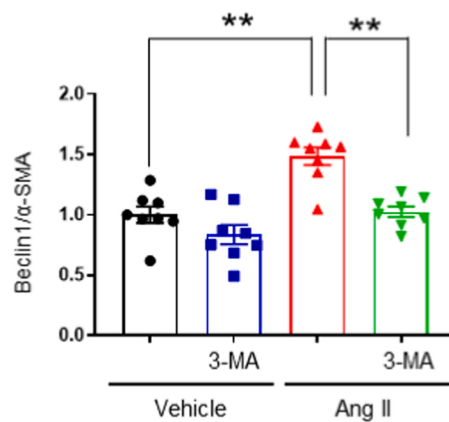
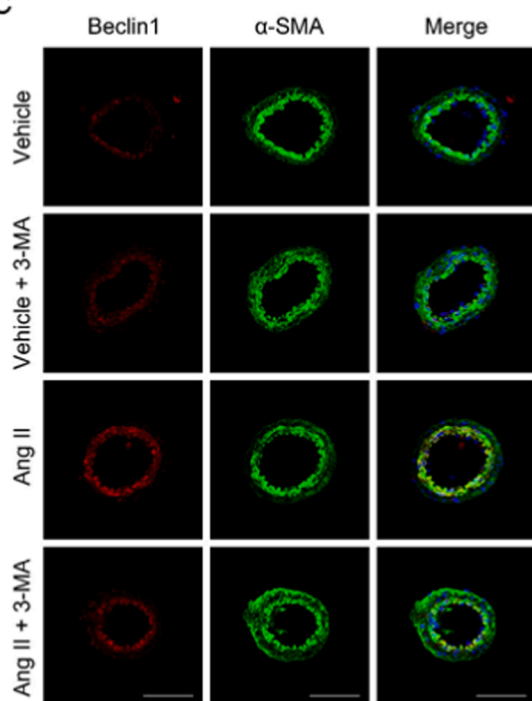
## A. Aortas



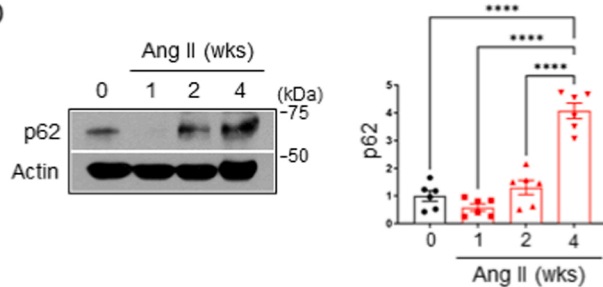
## B. Mesenteric arteries



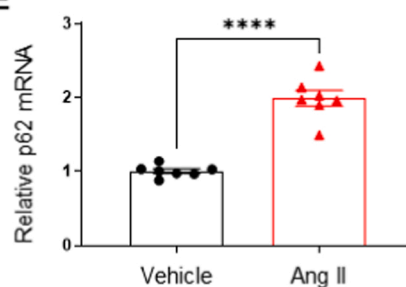
## C



## D



## E



(caption on next page)

**Fig. 2.** Effects of an autophagy inhibitor, 3-methyladenine, on the expression of autophagy markers in the aortas and mesenteric arteries of Ang II-induced hypertensive mice. (A and B) Western blot analysis data for beclin1, LC3, and p62 in vehicle- and Ang II-treated (with or without 3-methyladenine) mouse aortas (n = 7 for beclin1, n = 5 for LC3 and p62) and mesenteric arteries (n = 6 for beclin1, n = 5 for LC3 and p62). (C) Representative immunofluorescence images of the mesenteric arteries following treatment with vehicle and Ang II (with or without 3-methyladenine) and the graph represents the mean data for beclin1 expression (n = 8). Scale bar = 100  $\mu$ m. (D) Western blot analysis data for p62 expression following treatment with Ang II for various time periods (1, 2, and 4 weeks) and quantitative data for p62 (n = 6). (E) The graph represents the relative mRNA levels of p62 in the aortas from the mice infused with Ang II for 4 weeks (n = 7). Data are shown as means  $\pm$  SEM and are expressed as folds of control. The n-values mean number of animals. \* $p$  < 0.05, \*\* $p$  < 0.01, \*\*\* $p$  < 0.001, \*\*\*\* $p$  < 0.0001. (Veh: vehicle;  $\alpha$ -SMA:  $\alpha$ -smooth muscle actin).

dependent relaxation at the concentration of  $10^{-6}$  mol/L (Fig. 3D and E). Responses to SNP (nitric oxide donor) and eNOS inhibitor, L-NNA, were not different in all groups (Fig. 3F and G). The contraction responses to phenylephrine were not different among all groups (Fig. 3H).

### 3.4. Effect of 3-methyladenine on nitric oxide production in HUVECs and the mesenteric arteries

Since we observed treatment of 3-methyladenine significantly improved endothelium-dependent relaxation in the mesenteric arteries of Ang II-induced hypertensive mice, we measured nitric oxide level in the mesenteric arteries using DAF-FM diacetate, a fluorescent indicator for nitric oxide. The intensity for DAF-FM diacetate fluorescence was decreased in the mesenteric arteries from Ang II-treated mice, which was increased by treatment of 3-methyladenine (Fig. 4A). To strengthen *in vivo* data, we performed *in vitro* studies using HUVECs. We found that the levels of phosphorylated eNOS (p-eNOS) at S1177 were reduced by Ang II in cultured HUVECs ( $10^{-8}$ – $10^{-6}$  mol/L, Fig. 4B). Interestingly, treatment of 3-methyladenine to the HUVECs rescued the levels of p-eNOS (Fig. 4C). These data suggest that 3-methyladenine increases the production of nitric oxide in Ang II-induced hypertensive mice by regulating the levels of p-eNOS (S1177).

### 3.5. Direct effect of 3-methyladenine on the contractile responses in isolated mesenteric arteries

To further explore the effect of 3-methyladenine on vascular function, we observed direct effect of 3-methyladenine on the contractile responses in isolated mesenteric arteries. We applied 3-methyladenine to the isolated mesenteric arteries pre-contracted with PE ( $10^{-5}$  mol/L). As shown in the Fig. 5, 3-methyladenine concentration-dependently induced vasodilation in the mesenteric arteries. To confirm that 3-methyladenine induces same effect in the arteries pre-contracted with another vasoconstrictor, we applied U46619 ( $10^{-6}$  mol/L) into the isolated mesenteric arteries. We found that 3-methyladenine concentration-dependently induced vasodilation in U46619 pre-contracted arteries. To further explore the mechanism of 3-methyladenine induced vasodilation, we incubated the arteries with cyclooxygenase (COX) inhibitor, indomethacin ( $10^{-5}$  mol/L). The effect of 3-methyladenine was not different in the arteries incubated with indomethacin compared to the arteries without indomethacin (Fig. 5D and F). Treatment of L-NNA ( $5 \times 10^{-4}$  mol/L) significantly reduced vasodilation induced by 3-methyladenine (Fig. 5E and F). To confirm the effect of L-NNA, we observed vasodilatory effect of 3-methyladenine in endothelium denuded arteries using pressure myograph. We found that 3-methyladenine-induced vasodilation was significantly reduced in the endothelium-denuded arteries compared to endothelium-intact arteries (Fig. 5G–J). Fig. 5I shows that repetitive administration of U46619 ( $10^{-7}$  mol/L) induced similar vascular responses.

### 3.6. Ang II-induced changes in the expression levels of autophagic markers in vascular smooth muscle cells

In order to explore whether the increase in wall thickness in Ang II-treated mice is related with changes in VSMCs, we incubated rat aortic VSMCs with Ang II ( $10^{-8}$ – $10^{-6}$  mol/L) for 24 h. As Ang II induced increase in autophagy markers in aortas and mesenteric arteries, *in vitro*

treatment of Ang II induced increase in the expression levels of beclin1 and LC3 II in VSMCs (Fig. 6A). And treatment of Ang II decreased expression level of p62, which are inconsistent with our results of *in vivo* study. We also investigated the effect of 3-methyladenine in VSMCs. Treatment of Ang II ( $10^{-7}$  mol/L) significantly increased expression levels of beclin1 and LC3 II, which was reduced by treatment of 3-methyladenine. We observed treatment of 3-methyladenine significantly increased the expression level of p62 (Fig. 6B). To support the western blot data, we used alternative method to measure autophagy level. Acridine orange was used to stain acidic vesicular organelles which reflect late-stage autophagy. After 24 h of starvation, VSMCs were incubated with Ang II, 3-methyladenine or Ang II with 3-methyladenine for 24 h. As shown in Fig. 6C, Ang II enhanced intensity of acidic vesicular organelles, which was markedly reduced by 3-methyladenine.

## 4. Discussion

Autophagy is considered the new therapeutic target of various cardiovascular diseases such as pulmonary hypertension, atherosclerosis, and myocardial ischemia [14,29]. However, the involvement of autophagy in the pathogenesis of hypertension remains unclear. In the present study, we found that the inhibition of excessive autophagy ameliorates endothelial dysfunction in Ang II-induced hypertension. This is the first report on the effect of 3-methyladenine on systolic blood pressure and vascular functionality in resistance arteries. Our results indicate that (i) treatment of Ang II induces increase in autophagy, which is evidenced by the elevated levels of beclin1 and LC3 II; (ii) *in vivo* treatment of an autophagy inhibitor, 3-methyladenine, decreases blood pressure, induces a reduction in wall/lumen ratio, and improves endothelium-dependent relaxation by increasing nitric oxide production in rat mesenteric arteries.

Angiotensin II, an important hormone of the renin-angiotensin system (RAS), is known to induce vasoconstriction and increase blood pressure. Several *in vitro* studies have shown that Ang II induces autophagy in endothelial cells [19], vascular smooth muscle cells [20,21], cardiomyocytes [30], and podocytes [18,31]. It has been also reported that Ang II-infused mice exhibited enhanced autophagy [32,33]. In accordance with previous studies, our results show that treatment of Ang II induces increase in the expression levels of autophagy markers, beclin1 and LC3 II, in mesenteric arteries and aortas (Fig. 2) which is associated with elevated blood pressure and increase in wall thickness (Fig. 1). Interestingly, expression levels of p62 was increased in the mesenteric arteries and aortas from Ang II-infused mice, which was opposite result from what we expected. This phenomenon was not matched with the typical feature in which LC3 II and beclin1 are increased and p62 is decreased during autophagy. To identify the elevated levels of p62 in Ang II-treated mice, we measured the mRNA levels of p62 using quantitative RT-PCR. We found that chronic Ang II infusion induced p62 mRNA upregulation. Previous studies have shown that p62 is restored to basal levels during prolonged starvation, which depends on transcriptional upregulation [34]. The upregulation of p62 expression suggests adaptation to persistent starvation. This can be also explained by our *in vitro* result shows that 24 h of exposure to Ang II decreases expression level of p62 in VSMCs (Fig. 6A).

Although, it has been shown that an inhibitor of late-stage autophagy, chloroquine, has a relaxing effect on rat pulmonary arteries [35], rat aorta [36], and guinea pig trachea [37], there is no evidence that

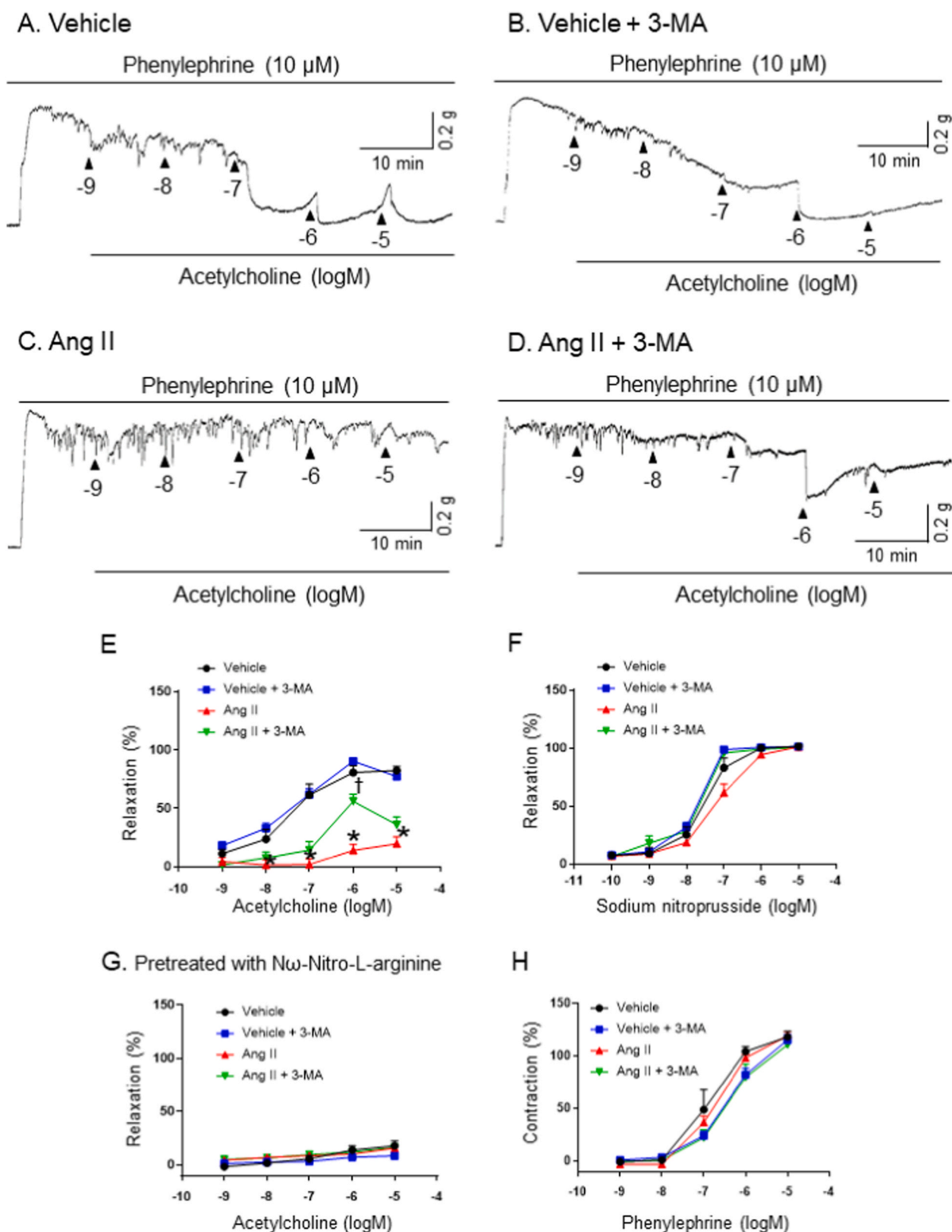


**Fig. 3.** Effects of an autophagy inhibitor, 3-methyladenine, on endothelium-dependent relaxation in the mesenteric arteries from Ang II-induced hypertensive mice. (A-D) Representative recordings of endothelium-dependent relaxation in response to acetylcholine ( $10^{-9}$ – $10^{-5}$  mol/L) on the vasoconstriction induced by phenylephrine ( $10^{-5}$  mol/L). (E) Mean data for endothelium-dependent relaxation ( $n = 11$  for Vehicle and Vehicle + 3-MA,  $n = 8$  for Ang II,  $n = 6$  for Ang II + 3-MA). (F) Mean data for sodium nitroprusside-induced vasorelaxation ( $n = 6$  for Vehicle and Ang II,  $n = 5$  for Vehicle + 3-MA,  $n = 7$  for Ang II + 3-MA). (G) Mean data for acetylcholine-induced vasorelaxation pretreated with L-NNA ( $n = 7$  for Vehicle,  $n = 5$  for Vehicle + 3-MA,  $n = 8$  for Ang II,  $n = 9$  for Ang II + 3-MA). (H) Mean data for phenylephrine-induced vasoconstriction ( $n = 4$  for Vehicle,  $n = 8$  for Vehicle + 3-MA, Ang II, and Ang II + 3-MA). Data are shown as means  $\pm$  SEM. The  $n$ -values mean number of vessels derived from each different animals. \* $p < 0.05$  for Vehicle vs. Ang II, † $p < 0.05$  for Ang II vs. Vehicle + 3-MA.

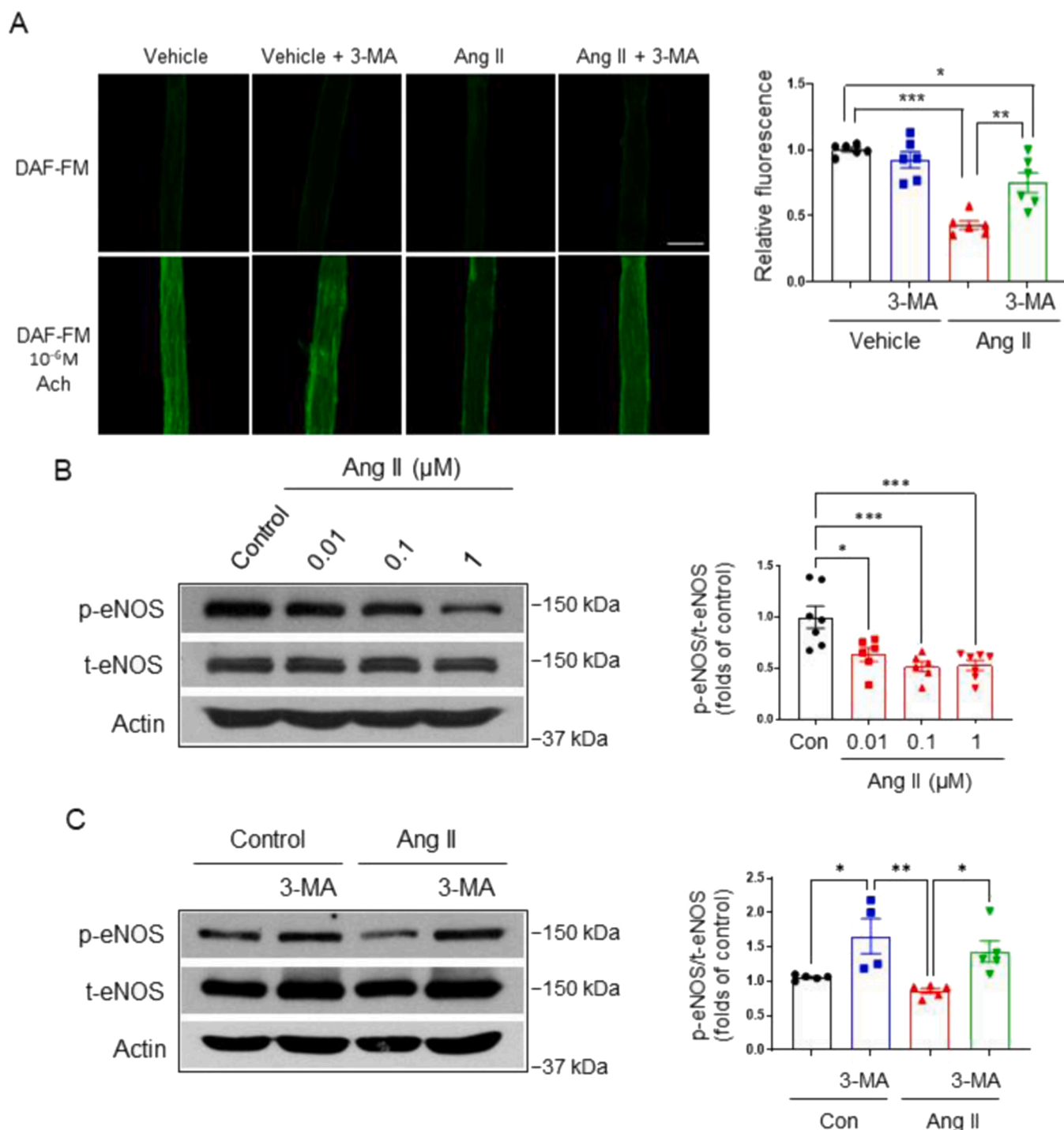


**Fig. 4.** Effects of an autophagy inhibitor, 3-methyladenine, on nitric oxide production in the mesenteric arteries and HUVECs. (A) Representative fluorescence images of mesenteric arteries incubated with DAF-FM diacetate ( $5 \times 10^{-6}$  mol/L) and statistical data for the relative fluorescence intensity ( $n = 6$ ). The effect of acetylcholine ( $10^{-6}$  M) on mesenteric arteries incubated with DAF-FM diacetate in Vehicle, Vehicle + 3-MA, Ang II, and Ang II + 3-MA groups. Scale bar = 200  $\mu$ m. (B) Western blot analysis data for p-eNOS (S1177) and total-eNOS with Ang II ( $10^{-8}$ – $10^{-6}$  mol/L) for 24 h. ( $n = 7$ ). (C) Western blot analysis data for p-eNOS (S1177) and total-eNOS expression following treatment with 3-methyladenine ( $5 \times 10^{-3}$  mol/L) and, Ang II ( $10^{-7}$  mol/L) or co-treatment with Ang II and 3-methyladenine for 24 h. ( $n = 5$ ). Data are shown as means  $\pm$  SEM and are expressed as folds of control. For nitric oxide detection, the n-values mean number of animals. \* $p < 0.05$ , \*\* $p < 0.01$  \*\*\* $p < 0.001$ . (3-MA: 3-methyladenine).

3-methyladenine, an inhibitor of early-stage autophagy, contributes to the arterial tone and regulation of blood pressure. In the present study, we demonstrated that in vivo treatment of 3-methyladenine reduced elevated blood pressure and wall thickness (Fig. 1), and improved endothelium-dependent relaxation in mesenteric resistance arteries of Ang II-induced hypertensive mice (Fig. 3). We found that relaxation

responses to nitric oxide donor, SNP, were not different in the arteries from all groups of mice. Furthermore, endothelium-dependent relaxation in the presence of eNOS inhibitor, L-NNA, were not different in the all groups of mice either. Thus we assume that the improved relaxation response of 3-methyladenine treated mice is dependent on endothelium especially eNOS. And there was no difference in contraction response to



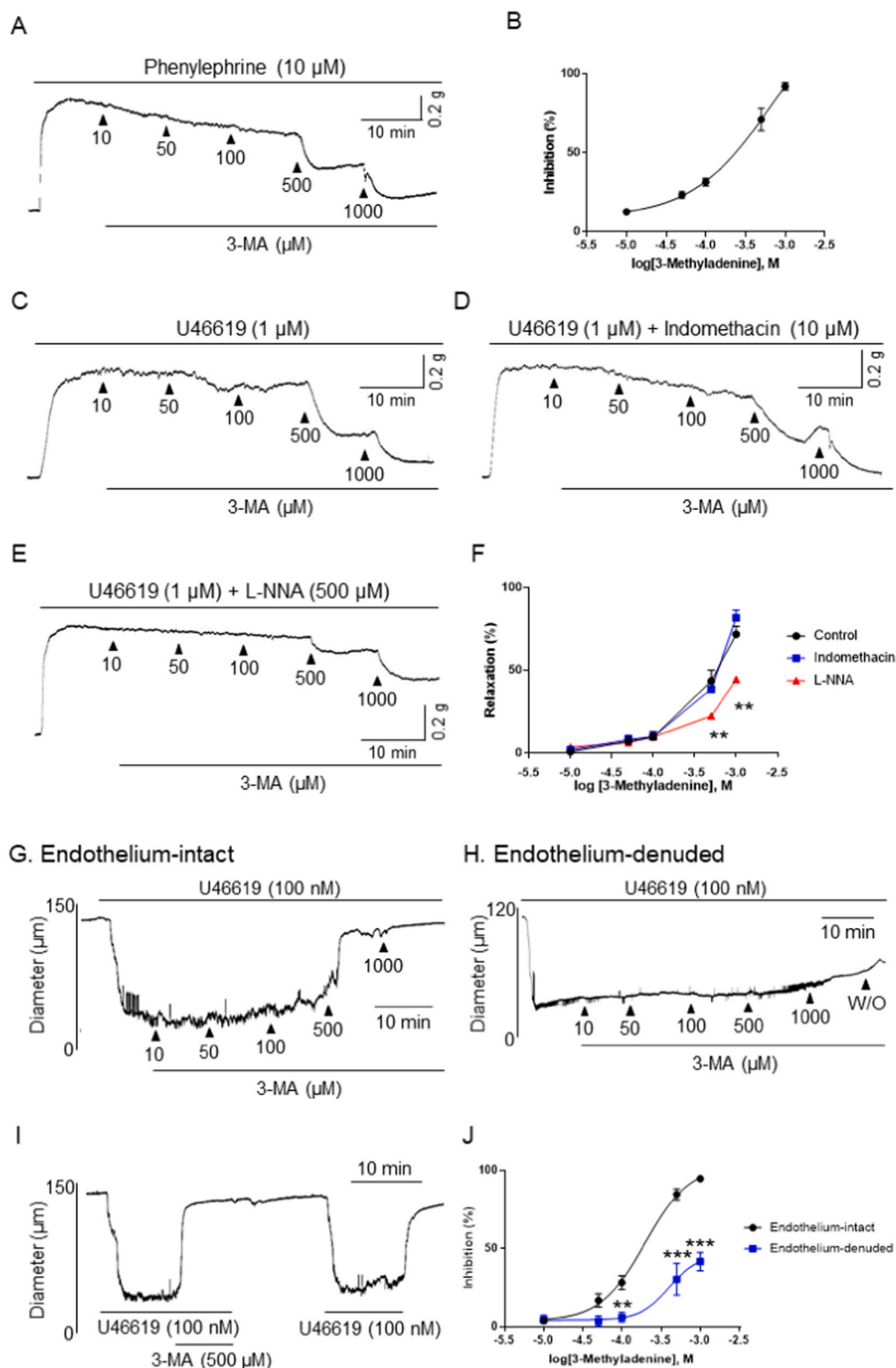


**Fig. 5.** Direct effects of an autophagy inhibitor, 3-methyladenine on the pre-contracted arteries. (A-B) Concentration-dependent responses to 3-methyladenine in mesenteric arteries pre-contracted with phenylephrine. (C-F) Effects of 3-methyladenine on the U46619-induced contraction in the presence or absence of indomethacin or L-NNA. ( $n = 7$ ) (G-J) Effects of 3-methyladenine on the U46619-induced contraction in endothelium-intact or endothelium-denuded mesenteric arteries. ( $n = 7$ ) Data are shown as means  $\pm$  SEM. The  $n$ -values mean number of vessels derived from each different animals. \*\* $p < 0.01$  for control vs. indomethacin or L-NNA. (L-NNA: N $\omega$ -nitro-L-arginine).

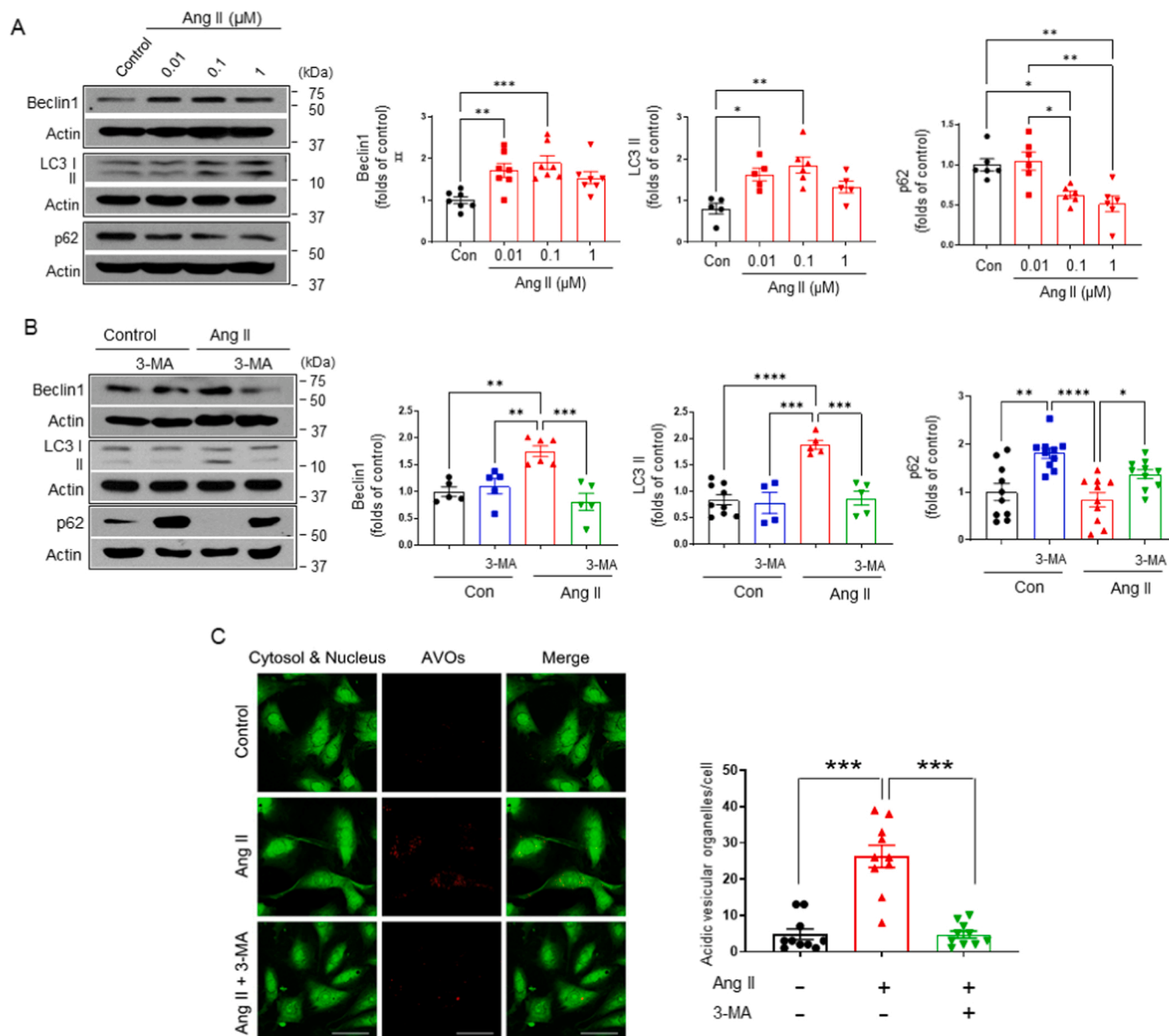


**Fig. 6.** Effects of an autophagy inhibitor, 3-methyladenine on the expression of autophagic markers in primary VSMCs. (A) Western blot analysis data showing the effect of Ang II on the expression levels of beclin1, LC3, and p62 in primary rat aortic VSMCs. (n = 7 for beclin1 and LC3, n = 6 for p62) (B) Western blot analysis data for beclin1, LC3, and p62 expression levels in primary rat aortic VSMCs treated with 3-methyladenine ( $5 \times 10^{-3}$  mol/L) or Ang II ( $10^{-7}$  mol/L) or co-treatment with Ang II and 3-methyladenine for 24 h. (n = 5 for beclin1 and LC3, n = 8 for p62) (C) Representative images of acridine orange-stained primary VSMCs following treatment with Ang II or co-treatment with Ang II and 3-methyladenine for 24 h and the graph represents the mean number of red puncta per cell. (Scale bar = 50 μm) The number of acidic vesicular organelles was counted from 10 randomly selected cells of 4 independent experiments and evaluated by Image J. Data are shown as means  $\pm$  SEM and are expressed as folds of control. \* $p < 0.05$ , \*\* $p < 0.01$ , and \*\*\* $p < 0.001$ , \*\*\*\* $p < 0.0001$ . (3-MA: 3-methyladenine;AVOs: acidic vesicular organelles).

PE in Ang II-induced hypertensive mice with or without 3-methyladenine.

To confirm the results of vascular reactivity study, we measured the phosphorylation levels of eNOS and nitric oxide production in mesenteric arteries using DAF-FM diacetate. Acetylcholine-induced nitric oxide production was decreased by treatment with Ang II, which was recovered by treatment with 3-methyladenine in mesenteric arteries (Fig. 4A). *In vitro* cell study also showed that the level of p-eNOS (S1177) decreased by treatment with Ang II, which was restored by treatment with 3-methyladenine in HUVECs. These results suggest that 3-methyladenine restores the activity of eNOS by phosphorylating eNOS (S1177). Therefore, we assume that 3-methyladenine improves endothelium-dependent relaxation by regulating nitric oxide production in Ang II-induced hypertension, which is evidenced by our data with

mesenteric arteries and HUVECs.

To confirm the effect of 3-methyladenine on the vascular function, we observed direct effect of 3-methyladenine on the contractile responses in isolated mesenteric arteries. 3-methyladenine concentration-dependently decreased U46619-induced and PE-induced contraction, which was significantly reduced by treatment of L-NNA or endothelium removal (Fig. 5). These data indicate that 3-methyladenine induces endothelium-dependent vascular relaxation in mesenteric arteries of mice. Nevertheless, our study could not rule out the possibility that 3-methyladenine may cause vascular relaxation regardless of autophagy mechanism. However, previous study from other group showed that treatment of 3-methyladenine and siLC3 (small interfering RNA against LC3) reduced elevated blood pressure in spontaneously hypertensive rats, which provides the evidence that autophagy inhibitors have direct

effect on hypertension [22]. In-depth follow-up studies are needed to identify this mechanism.

Previously, we demonstrated that wall thickness was increased in the mesenteric arteries from Ang II-treated mice, which was reduced by treatment of 3-methyladenine (Fig. 1). These results could be related with the changes in arterial smooth muscle cells. Thus we investigated the changes in expression levels of autophagy markers upon treatment of Ang II and whether treatment of 3-methyladenine affects expression levels of autophagy markers. We found that Ang II increased the expression levels of beclin1 and LC3 II whereas decreased p62 (Fig. 6). And acidic vesicular organelles which reflect late-stage autophagy was markedly increased in Ang II-treated VSMCs, which was almost normalized by 3-methyladenine. These results are consistent with previous study showed that inhibition of autophagy with 3-methyladenine resulted in inhibition of smooth muscle cell proliferation in mouse common carotid arteries [38].

## 5. Conclusion

In summary, we suggest that excessive autophagy is involved in the progression of Ang II-induced hypertension. The inhibition of autophagy with 3-methyladenine improves endothelial function by regulating eNOS phosphorylation, which is associated with reduction in elevated blood pressure in Ang II-induced hypertension.

## Funding

This work was supported by the National Research Foundation of Korea (NRF) with funding from the Ministry of Education, Science and Technology granted to S.-K.C. (2018R1D1A1B07041820) and Y.-H.L. (2019R1F1A1061771). The funders had no role in study design, data collection and analysis, decision to publish, or preparation of the manuscript.

## Author contributions

All the work was done in the laboratory of Y.-H. L. in the department of physiology at Yonsei University College of Medicine. Y.K. designed the experiments, contributed data acquisition, and wrote the manuscript. C.E.H and S.B. performed the western blot analysis. Y.-H. L. and S.-K.C. contributed to the analysis and interpretation of the data and revised the work critically. All authors approved the final version of the manuscript, all persons designated as authors qualify for authorship, and all those who qualify for authorship are listed.

## CRediT authorship contribution statement

**Youngin Kwon:** Conceptualization, Methodology, Investigation, Software, Writing – original draft. **Chae Eun Haam:** Validation, Reviewing. **Seonhee Byeon:** Investigation, Software, Validation. **Soo-Kyoung Choi:** Conceptualization, Writing – original draft, Writing – review & editing, Supervision. **Young-Ho Lee:** Writing – review & editing, Supervision.

## Conflict of interest statement

The authors declare that the research was conducted in the absence of any commercial or financial relationships that could be construed as a potential conflict of interest.

## Data Availability

Data will be made available on request.

## References

- [1] B. Zhou, P. Perel, G.A. Mensah, M. Ezzati, Global epidemiology, health burden and effective interventions for elevated blood pressure and hypertension, *Nat. Rev. Cardiol.* 18 (2021) 785–802.
- [2] R.S. de Lima, J.C.S. Silva, C.T. Lima, L.E. de Souza, M.B. da Silva, M.G. Baladi, et al., Proinflammatory role of angiotensin II in the aorta of normotensive mice, *Biomed. Res. Int.* 2019 (2019), 9326896.
- [3] S.K. Choi, M. Lim, S.I. Yeon, Y.H. Lee, Inhibition of endoplasmic reticulum stress improves coronary artery function in type 2 diabetic mice, *Exp. Physiol.* 101 (2016) 768–777.
- [4] R.P. Brandes, Endothelial dysfunction and hypertension, *Hypertension* 64 (2014) 924–928.
- [5] B. Levine, G. Kroemer, Autophagy in the pathogenesis of disease, *Cell* 132 (2008) 27–42.
- [6] S.M. Hill, L. Wrobel, D.C. Rubinshtein, Post-translational modifications of beclin 1 provide multiple strategies for autophagy regulation, *Cell Death Differ.* 26 (2019) 617–629.
- [7] Y. Mei, M.D. Thompson, R.A. Cohen, X. Tong, Autophagy and oxidative stress in cardiovascular diseases, *Biochim. Biophys. Acta* 1852 (2015) 243–251.
- [8] P. Ravanan, I.F. Srikumar, P. Talwar, Autophagy: the spotlight for cellular stress responses, *Life Sci.* 188 (2017) 53–67.
- [9] Y.T. Wu, H.L. Tan, G. Shui, C. Bauvy, Q. Huang, M.R. Wenk, et al., Dual role of 3-methyladenine in modulation of autophagy via different temporal patterns of inhibition on class I and III phosphoinositide 3-kinase, *J. Biol. Chem.* 285 (2010) 10850–10861.
- [10] Y. Tu, C. Guo, F. Song, Y. Huo, Y. Geng, M. Guo, et al., Mild hypothermia alleviates diabetes aggravated cerebral ischemic injury via activating autophagy and inhibiting pyroptosis, *Brain Res. Bull.* 150 (2019) 1–12.
- [11] A. Zhang, Y. Song, Z. Zhang, S. Jiang, S. Chang, Z. Cai, et al., Effects of autophagy inhibitor 3-methyladenine on ischemic stroke: a protocol for systematic review and meta-analysis, *Medicine* 100 (2021), e23873.
- [12] S.A. Slavin, A. Leonard, V. Grose, F. Fazal, A. Rahman, Autophagy inhibitor 3-methyladenine protects against endothelial cell barrier dysfunction in acute lung injury, *Am. J. Physiol. Lung Cell. Mol. Physiol.* 314 (2018) L388–L396.
- [13] N.T. Cheng, H. Meng, L.F. Ma, L. Zhang, H.M. Yu, Z.Z. Wang, et al., Role of autophagy in the progression of osteoarthritis: the autophagy inhibitor, 3-methyladenine, aggravates the severity of experimental osteoarthritis, *Int. J. Mol. Med.* 39 (2017) 1224–1232.
- [14] Z.V. Wang, B.A. Rothermel, J.A. Hill, Autophagy in hypertensive heart disease, *J. Biol. Chem.* 285 (2010) 8509–8514.
- [15] C.G. McCarthy, C.F. Wenceslau, F.B. Calmasini, N.S. Klee, M.W. Brands, B. Joe, et al., Reconstitution of autophagy ameliorates vascular function and arterial stiffening in spontaneously hypertensive rats, *Am. J. Physiol. Heart Circ. Physiol.* 317 (2019) H1013–H1027.
- [16] E.R. Porrello, A. D'Amore, C.L. Curl, A.M. Allen, S.B. Harrap, W.G. Thomas, et al., Angiotensin II type 2 receptor antagonizes angiotensin II type 1 receptor-mediated cardiomyocyte autophagy, *Hypertension* 53 (2009) 1032–1040.
- [17] S. Liu, S. Chen, M. Li, B. Zhang, P. Shen, P. Liu, et al., Autophagy activation attenuates angiotensin II-induced cardiac fibrosis, *Arch. Biochem. Biophys.* 590 (2016) 37–47.
- [18] A. Yadav, S. Vallabu, S. Arora, P. Tandon, D. Slahan, S. Teichberg, et al., Ang II promotes autophagy in podocytes, *Am. J. Physiol. Cell Physiol.* 299 (2010) C488–C496.
- [19] F. Chen, B. Chen, F.Q. Xiao, Y.T. Wu, R.H. Wang, Z.W. Sun, et al., Autophagy protects against senescence and apoptosis via the ras-mitochondria in high-glucose-induced endothelial cells, *Cell Physiol. Biochem.* 33 (2014) 1058–1074.
- [20] K.Y. Yu, Y.P. Wang, L.H. Wang, Y. Jian, X.D. Zhao, J.W. Chen, et al., Mitochondrial katp channel involvement in angiotensin II-induced autophagy in vascular smooth muscle cells, *Basic Res. Cardiol.* 109 (2014) 416.
- [21] D. Mondaca-Ruff, J.A. Riquelme, C. Quiroga, I. Norambuena-Soto, F. Sanhueza-Olivares, P. Villar-Fincheira, et al., Angiotensin II-regulated autophagy is required for vascular smooth muscle cell hypertrophy, *Front. Pharmacol.* 9 (2018) 1553.
- [22] Y.M. Chao, M.D. Lai, J.Y. Chan, Redox-sensitive endoplasmic reticulum stress and autophagy at rostral ventrolateral medulla contribute to hypertension in spontaneously hypertensive rats, *Hypertension* 61 (2013) 1270–1280.
- [23] S. Dai, B. Wang, W. Li, L. Wang, X. Song, C. Guo, et al., Systemic application of 3-methyladenine markedly inhibited atherosclerotic lesion in apoE(-/-) mice by modulating autophagy, foam cell formation and immune-negative molecules, *Cell Death Dis.* 7 (2016), e2498.
- [24] S.K. Choi, M. Lim, S.H. Byeon, Y.H. Lee, Inhibition of endoplasmic reticulum stress improves coronary artery function in the spontaneously hypertensive rats, *Sci. Rep.* 6 (2016) 31925.
- [25] G. SenthilKumar, J.H. Skiba, R.J. Kimple, High-throughput quantitative detection of basal autophagy and autophagic flux using image cytometry, *Biotechniques* 67 (2019) 70–73.
- [26] S.I. Yeon, J.Y. Kim, D.S. Yeon, J. Abramowitz, L. Birnbaumer, S. Muallem, et al., Transient receptor potential canonical type 3 channels control the vascular contractility of mouse mesenteric arteries, *PLoS One* 9 (2014), e110413.
- [27] J.Y. Wang, Q. Xia, K.T. Chu, J. Pan, L.N. Sun, B. Zeng, et al., Severe global cerebral ischemia-induced programmed necrosis of hippocampal ca1 neurons in rat is prevented by 3-methyladenine: a widely used inhibitor of autophagy, *J. Neuropathol. Exp. Neurol.* 70 (2011) 314–322.
- [28] Y. Liu, D. Li, Z. He, Q. Liu, J. Wu, X. Guan, et al., Inhibition of autophagy-attenuated calcium oxalate crystal-induced renal tubular epithelial cell injury in vivo and in vitro, *Oncotarget* 9 (2018) 4571–4582.

- [29] S. Tai, X.Q. Hu, D.Q. Peng, S.H. Zhou, X.L. Zheng, The roles of autophagy in vascular smooth muscle cells, *Int. J. Cardiol.* 211 (2016) 1–6.
- [30] L. Lin, X. Liu, J. Xu, L. Weng, J. Ren, J. Ge, et al., Mas receptor mediates cardioprotection of angiotensin-(1-7) against angiotensin ii-induced cardiomyocyte autophagy and cardiac remodelling through inhibition of oxidative stress, *J. Cell Mol. Med.* 20 (2016) 48–57.
- [31] N. Mao, R.Z. Tan, S.Q. Wang, C. Wei, X.L. Shi, J.M. Fan, et al., Ginsenoside rg1 inhibits angiotensin ii-induced podocyte autophagy via ampk/mtor/pi3k pathway, *Cell Biol. Int.* 40 (2016) 917–925.
- [32] Q. Shen, X. Bi, L. Ling, W. Ding, 1,25-dihydroxyvitamin d3 attenuates angiotensin ii-induced renal injury by inhibiting mitochondrial dysfunction and autophagy, *Cell. Physiol. Biochem.* 51 (2018) 1751–1762.
- [33] Z. Cheng, M. Zhang, J. Hu, J. Lin, X. Feng, S. Wang, et al., Mst1 knockout enhances cardiomyocyte autophagic flux to alleviate angiotensin ii-induced cardiac injury independent of angiotensin ii receptors, *J. Mol. Cell Cardiol.* 125 (2018) 117–128.
- [34] M.H. Sahani, E. Itakura, N. Mizushima, Expression of the autophagy substrate sqstm1/p62 is restored during prolonged starvation depending on transcriptional upregulation and autophagy-derived amino acids, *Autophagy* 10 (2014) 431–441.
- [35] K. Wu, Q. Zhang, X. Wu, W. Lu, H. Tang, Z. Liang, et al., Chloroquine is a potent pulmonary vasodilator that attenuates hypoxia-induced pulmonary hypertension, *Br. J. Pharmacol.* 174 (2017) 4155–4172.
- [36] P.I. Aziba, D.T. Okpako, Effects of chloroquine on smooth muscle contracted with noradrenaline or high-potassium solutions in the rat thoracic aorta, *J. Smooth Muscle Res.* 39 (2003) 31–37.
- [37] V. Pulkkinen, M.L. Manson, J. Safholm, M. Adner, S.E. Dahlen, The bitter taste receptor (tas2r) agonists denatonium and chloroquine display distinct patterns of relaxation of the guinea pig trachea, *Am. J. Physiol. Lung Cell. Mol. Physiol.* 303 (2012) L956–L966.
- [38] H. Li, J. Li, Y. Li, P. Singh, L. Cao, L.J. Xu, et al., Sonic hedgehog promotes autophagy of vascular smooth muscle cells, *Am. J. Physiol. Heart Circ. Physiol.* 303 (2012) H1319–H1331.